The magnitude of airway remodelling is not altered by distinct allergic inflammatory responses in BALB/c vs C57BL/6 mice, but matrix composition differs

James E Parkinson[1,2], Stella Pearson[1,2], Dominik Rückerl[1], Judith E Allen[1,2], Tara E Sutherland*[1]

[1]Lydia Becker Institute for Immunology and Infection, Faculty of Biology, Medicine and Health, Manchester Academic Health Science Centre, University of Manchester, Manchester, United Kingdom

[2]Wellcome Centre for Cell-Matrix Research, Faculty of Biology, Medicine and Health, Manchester Academic Health Science Centre, University of Manchester, Manchester, United Kingdom

*Corresponding Author
Tara E Sutherland
The University of Manchester, Core Technology Facility, 46 Grafton St, Manchester, M13 9NT
tara.sutherland@manchester.ac.uk
Phone: +44 (0)161 306 6052

Running title:
Allergic airway inflammation and remodelling in mice

Key words:
Allergic airway inflammation; type 2 cytokines; type 17 cytokines; extracellular matrix; airway remodelling; collagen; mouse strain variation

Abstract

Airway inflammation in response to allergens is heterogenous with variability in immune phenotypes observed across asthmatic patients. Whilst inflammation, specifically type 2 immune responses, are thought to directly contribute to airway remodelling and pathology in asthma, clinical data suggests that neutralising type 2 cytokines do not necessarily alter disease pathogenesis. Here we show, using a mouse model allergic airway inflammation, that both C57BL/6 and BALB/c mice develop mixed type 2 and type 17 inflammation. However, BALB/c mice develop much greater inflammatory responses than C57BL/6 mice, effects possibly explained by a reduction in pathways that regulate and maintain T cell activation in C57BL/6 mice, as shown by RNA transcript analysis. Chronic allergen exposure resulted in a similar degree of airway remodelling changes such as ECM deposition and increases in goblet cells and airway muscle mass between mouse strains. However, collagen subtype composition revealed increased collagen III around of the airways of C57BL/6 but not BALB/c mice. Furthermore, allergen-induced loss of basement membrane collagen IV was only observed in BALB/c mice. This study highlights a model of type 2/type 17 airway inflammation in mice whereby development of airway remodelling can occur in both BALB/c and C57BL/6 mice despite differences in immune response dynamics between strains. Importantly, compositional differences in the ECM between genetic strains of mice may help us better understand the relationships between lung function, remodelling and airway inflammation.

Introduction

Asthma is a global health problem with increasing prevalence, currently affecting over 300 million people[1]. Of note, the term "asthma" encompasses a range of disease phenotypes. Progress in understanding heterogeneity of airway inflammation has led to defined asthma endotypes[2,3] often characterized by the presence or absence of type 2 eosinophilic inflammation and/or type 17 neutrophilic inflammation[4]. A clarified definition of such inflammatory phenotypes in asthma has led to development of innovative therapies targeting specific inflammatory pathways, in particular type 2 inflammation[5]. Whilst the use of biologicals targeting IgE or type 2 cytokines IL-5, IL-4, IL-13 have been effective at reducing disease exacerbations in allergic asthmatics, these therapies are often insufficient to improve underlying disease pathogenesis[6-8]. Furthermore, clinical trials with antibodies targeting IL-17 signalling have shown no benefit[9], despite a strong association of severe asthma with type 17 neutrophilic inflammation[10]. In fact, neutrophils, whilst generally considered pathogenic in severe asthma, are increasingly recognized for a protective and regulatory role in asthma[11] and models of allergic airway inflammation[12]. To achieve progress in treating asthma we need a more comprehensive understanding of pathology beyond viewing inflammation as the main instigator of disease.

Along with airway inflammation, asthma is characterized by airway hyper-responsiveness (AHR) and airway remodelling, a process of changes to the composition, content and organisation of cells and extracellular matrix in the lung. Whilst tissue remodelling is a critical process during development and tissue repair[13], it is also a pathogenic response in diseases like asthma, and undoubtedly impacts on lung function[14]. Comprehensive research using a combination of mouse models and human studies typically attribute the development of remodelling to chronic airway inflammation[15-19]. However, this view conflicts with emerging data that shows remodelling can occur as a primary event prior to inflammation[20-22], or that anti-inflammatory drugs that successfully target specific inflammatory pathways, fail to improve lung function[7,8] presumably because they do not affect airway remodelling. Airway remodelling is a complex disease process, difficult to study in patients especially in the context of understanding multiple components that may influence development of individual remodelling processes over time. Therefore, there is a

crucial need for animal models that reflect asthma disease processes with a focus on studying the development of stable and irreversible airway remodelling.

Genetic differences between inbred mouse strains are well known to strongly affect both airway inflammation [23-26] and AHR[27]. For instance, C57BL/6 mice are known to have a high airway resistance in response to methacholine challenge independent of allergic inflammation[23], whereas BALB/c mice generally exhibit greater airway reactivity in response to allergens[27]. Therefore, studies examining airway pathology in different mouse strains can provide a basis to explore the relationships between immune cell dynamics in relation to changes in airway remodelling and lung function. In this study we utilised a model of chronic allergic airway inflammation that shares features of disease common to severe asthma in people, including mixed type 2 and type 17 airway inflammation, steroid resistant neutrophilia and AHR independent of type 2 cytokines[28,29]. Our results revealed exaggerated type 2 and type 17 pulmonary allergen-induced immune responses in BALB/c compared to C57BL/6 mice. Despite these differences in inflammation, chronic allergen exposure increased collagen deposition, airway smooth muscle mass and goblet cell hyperplasia in both mouse strains, indicating a similar degree of airway remodelling. However, more detailed examination of the extracellular matrix (ECM) around the airways showed differences in collagen subtype composition between BALB/c and C57BL/6 mice. Together, these results describe an allergic airway pathology model whereby mouse strain dependent differences in type 2 and type 17 inflammation do not seem to alter the development of remodelling but may impact on deposition of specific collagen subtypes.

Results

Chronic allergen-induced immune response dynamics differ between C57BL/6 and BALB/c mouse strains.

Aspects of allergen-induced airway inflammation have been extensively studied in mouse models, largely in the context of acute Th2-mediated immune responses[30,31]. Here, using a model of mixed type 2 and type 17 inflammation, we characterised immune cell dynamics in two common in-bred mouse strains, C57BL/6 and BALB/c, strains known to respond differently in models of airway inflammation and hyper-responsiveness[27,32,33]. Mice were exposed to a multi-allergen cocktail (House Dust Mite, Ragweed and *Aspergillus fumigatus*; DRA) for 4 or 8 weeks (**Fig 1a**) and inflammation assessed. All mice exposed to DRA had a mixed neutrophilic/eosinophilic inflammation, although neutrophilia was not evident in C57BL/6 mice until week 8 (**Fig 1b**). Neutrophils were still present in the BAL 5 days after the last allergen administration, even if their numbers were considerably lower compared to eosinophils. Analysis of T lymphocyte and related populations in the lungs, revealed relatively similar proportions of allergen-induced immune cell accumulation between mouse strains, with gradual increases in ILCs (**Fig 1c**). BALB/c mice generally had a greater ratio of CD4+ to CD8+ T cells compared to C57BL/6 mice but this did not change due to allergen exposure (**Fig 1c**). In addition, innate populations of γδT cells and innate lymphoid cells (ILCs) were also more predominant in BALB/c mice compared to C57BL/6 mice (**Fig 1c**). Regardless, $CD4^+$ T cells and γδT cells appeared to be the major cytokine producing lymphocyte populations in the lungs of all allergic mice. Exposure to DRA resulted in both IL-17A and type 2 inflammatory responses in the lung, with an increased proportion of IL-4 and IL-17A expressing $CD4^+$ T cells in both C57BL/6 and BALB/c mice (**Fig 2a**). Interestingly, the numbers of IL-4^+ $CD4^+$ T cells were reduced from week 4 to week 8 in BALB/c mice (**Fig 2b**), also corresponding to a reduction in eosinophils (**Fig 1b**), perhaps reflecting the emergence of a tolerogenic response to allergens in BALB/c mice[26]. Nonetheless, there were enhanced numbers of IL-$17A^+$ TCRγδ^+ T cells and IL-$17A^+$ $CD4^+$ T as well as IL-4^+ $CD4^+$ T cells on week 4 in BALB/c compared to C57BL/6 mice (**Fig 2b**). Interestingly, TCRγδ^+ and $CD4^+$ T cells contributed equally to the pool of IL-$17A^+$ cells in allergic BALB/c mice, whereas $CD4^+$ T cells were the main IL-$17A^+$ population in C57BL/6 mice (**Fig 2b**).

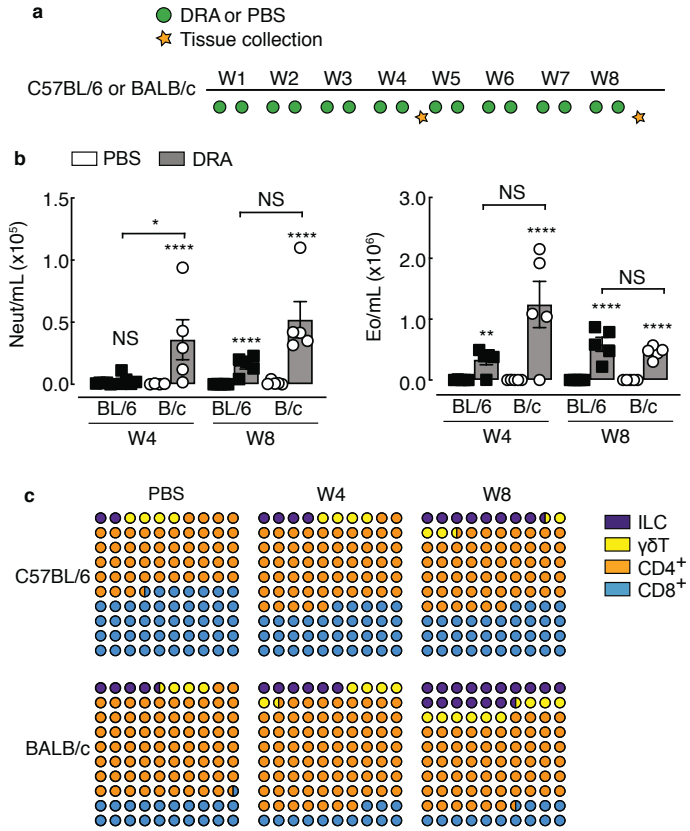

Figure 1: Chronic exposure to DRA allergens induced neutrophil and eosinophil airway inflammation
a) Schematic showing allergic airway inflammation model highlighting the timing of DRA or PBS intranasal administration into C57BL/6 or BALB/c mice. Cells were collected for flow cytometry analysis 5 days after the last administration of PBS or DRA at either 4 or 8 weeks. **b**) Numbers of neutrophils and eosinophils in the BAL of C57BL/6 or BALB/c mice administered PBS or DRA for 4 or 8 weeks. **c**) Plot showing the average proportions of different T cells and ILCs in the lungs of C57BL/6 or BALB/c mice administered PBS or DRA for 4 or 8 weeks. Data are representative of 2 experiments. Data is plotted as mean ± sem with points representing individual animals (**b**). Data was analysed by ANOVA with Tukey's multiple comparison test with significance level showing comparisons between either PBS animals within each strain and each time point or C57BL/6 to BALB/c mice as indicated on the graph. NS not significant, *P<0.05, ****P<0.0001.

Expression of key cytokines in whole lung RNA also revealed an increase in type 2 and *Il17a* genes upon DRA treatment with exaggerated *Il13* and *Il17a* expression at week 4 in allergic BALB/c compared to C57BL/6 mice (**Fig 2c**). Whilst we saw no evidence of increased IFNγ$^+$ T cells or ILCs (data not shown) in the lungs of mice following allergen administration, there was a transient increase in *Ifng* expression in the lungs of C57BL/6 mice but not BALB/c (**Fig 2c**). Overall, although both mouse strains developed allergen-induced airway inflammation, the degree of inflammation and eosinophilic and neutrophilic responses were higher in BALB/c compared to C57BL/6 mice.

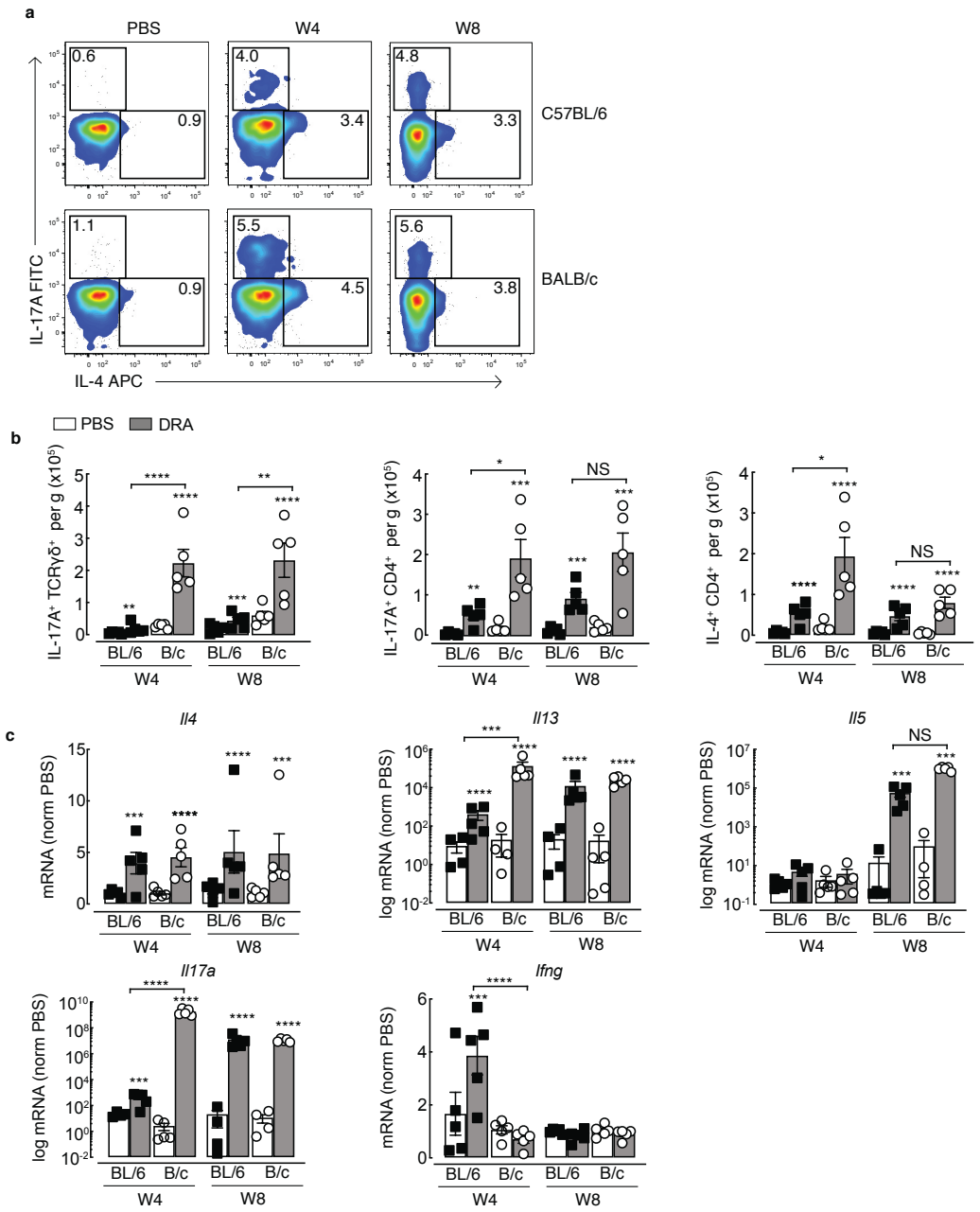

Figure 2: Chronic exposure to DRA allergens induce mixed Th2/Th17 airway inflammation

a) Representative intracellular staining of IL-4$^+$ and IL-17A$^+$ CD4$^+$ T cells in the lungs of C57BL/6 or BALB/c mice administered PBS or DRA intranasally two times a week for up to 8 weeks. Cells were analysed by flow cytometry 5 days after the last inoculation. Single cell lung suspensions were stimulated with PMA/ionomycin prior to analysis by flow cytometry. Numbers indicate the percentage of cytokine positive CD4$^+$ T cells within each gate. **b**) Absolute numbers of IL-17A$^+$ TCRγδ$^+$ or IL-17A$^+$ or IL-4$^+$ CD4$^+$ T cells in the lungs of mice as in **a**. **c**) mRNA expression of *Il4*, *Il13*, *Il5*, *Il17a* and *Ifng* in whole lungs of mice treated as in **a.** mRNA were normalised to levels found in PBS C57BL/6 or BALB/c mice at each time point and are relative to geometric mean of housekeeping genes *Gapdh*, *Rpl13a* and *Rn45s.* Data are representative of 2 experiments. Data is plotted as mean ± sem with points representing individual animals. Data was analysed by ANOVA with Tukey's multiple comparison test with significance level showing comparisons between either PBS animals within each strain and each time point or C57BL/6 to BALB/c mice as indicated on the graph. NS not significant, **P*<0.05, ***P*<0.01, ****P*<0.001, *****P*<0.0001.

Chitinase-like proteins are abundantly expressed in the lungs during type 2 and type 17 allergic airway inflammation

Chitinase-like proteins (CLPs) are molecules strongly associated with severe asthma, neutrophilia and IL-17A[34-37]. Following exposure to DRA allergen, expression of murine CLPs *Chil1* (BRP-39), *Chil3* (Ym1) and *Chil4* (Ym2) were upregulated in both BALB/c and C57BL/6 mice compared to PBS controls (**Fig 3a**). However, *Chil1* expression was markedly less in C57BL/6 compared to BALB/c mice and was not altered at week 4 in C57BL/6 mice (**Fig 3a**) despite significant increases in secreted BRP-39 levels in the BAL (**Fig 3b**). *Chil3* and *Chil4* were significantly increased in both mouse strains at week 4, and expression levels did not change upon further allergen exposure (**Fig 3a**), findings that were supported by measurement of Ym1 secreted protein in the BAL (**Fig 3b**). As there were no commercially available reagents to measure Ym2 protein levels, we developed a Ym2 specific antibody to examine Ym2 expression in the lungs (**Sup Fig 1**). By western blot, neither Ym1 nor Ym2 was detected in mice administered PBS, but both Ym1 and Ym2 greatly increased following allergen exposure (**Fig 3c**), mirroring results obtained by ELISA. CLPs can be readily detected in the serum, and serum levels of YKL-40 in humans has been proposed as a biomarker for disease severity and associated with reduced lung function in several pulmonary pathologies[38-40]. Although BRP-39 is a genetic ortholog of YKL-40, the level of BRP-39 in the blood was not significantly altered following allergic-inflammation in this model (**Fig 3d**). However, increased serum Ym1 was detectable in allergic mice of both strains (**Fig 3d**). To determine whether localisation of the three CLPs differed between strains of mice following allergen exposure, we examined immunostained lung sections. BRP-39 was already expressed in macrophages and epithelial cells in the steady state, but the intensity and number of positive cells increased further following allergen administration and the increase was particularly evident in BALB/c mice (**Fig 3e**). Corresponding to secreted levels in the BAL (**Fig 3c**), expression of Ym2 was absent in the lungs of PBS mice, but there were numerous $Ym1^{+}$ cells, likely alveolar macrophages (**Fig 3f**) [41]. The expression of Ym1 and Ym2 dramatically increased in the lungs of allergic BALB/c or C57BL/6 mice and the level of expression reached maximal expression at 4 weeks post DRA treatment (**Fig 3f**). Interestingly, Ym1 and Ym2 appear to have a fairly distinct expression pattern in the lung, with Ym1 largely restricted to myeloid cells and Ym2 largely expressed by epithelial cells (**Fig 3f & 3g**). Whilst there were a few cells that co-stained for Ym1 and Ym2 (**Fig 3g**), the

different staining patterns suggest a possible divergent transcriptional activation of these two highly homologous proteins and potentially varying functions. Overall, we observed modest increases in BRP-39 levels in allergic animals, but strongly enhanced Ym1 and Ym2 expression in the lungs of both allergic C57BL/6 and BALB/c mice. For the first time we show distinct expression of Ym2 in the lungs compared to Ym1, despite their protein sequence being ~96% homologous.

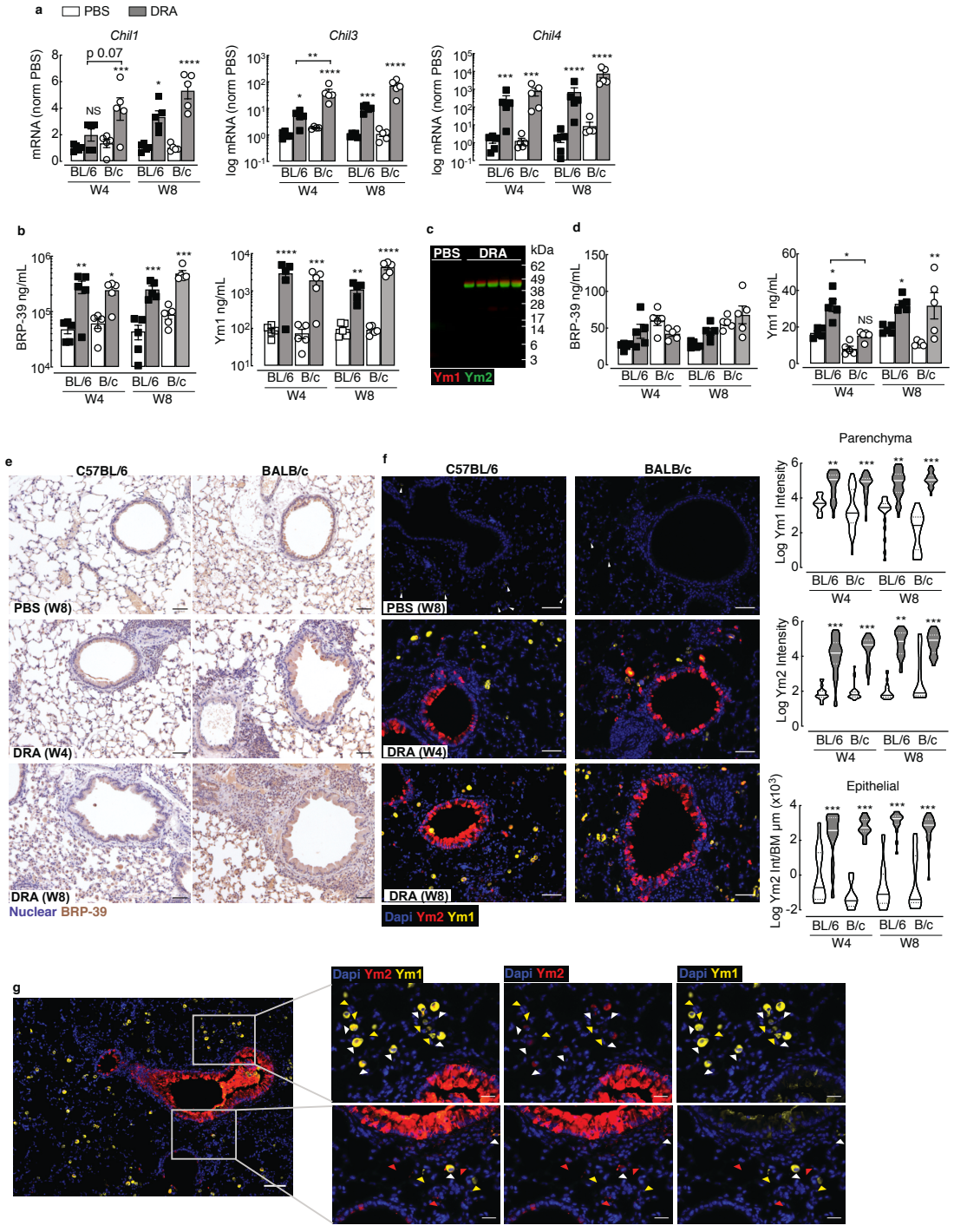

Figure 3: Chitinase-like proteins are abundantly expressed during chronic allergic airway inflammation

a) mRNA expression of CLPs *Chil1*, *Chil3* and *Chil4* in whole lungs of C57BL/6 or BALB/c mice exposed intranasally to PBS or DRA for 4 or 8 weeks. Lungs were collected 5 days after the last PBS/DRA administration. mRNA were normalised to levels found in PBS C57BL/6 or BALB/c mice at each time point and are relative to the geometric mean of housekeeping genes *Gapdh*, *Rpl13a* and *Rn45s*. *Chil3* and *Chil4* is depicted as log mRNA levels. **b**) Concentration of Ym1 and BRP-39 measured by ELISA in the BAL of C57BL/6 or BALB/c mice treated as in **a**. **c**) Western blot analysis of Ym1 (red) and Ym2 (green) levels in the BAL from C57BL/6 mice administered with PBS or DRA for 8 weeks, with BAL taken 5 days after the last DRA/PBS administration. **e**) Concentration of Ym1 and BRP-39 measured by ELISA in serum of C57BL/6 or BALB/c mice treated as in **a**. **e**) Microscopy images of immunohistochemical staining of BRP-39 (brown) in lung sections from C57BL/6 and BALB/c mice treated with either PBS for 8 weeks, or DRA for 4 or 8 weeks. Cell nuclei counterstained with haematoxylin (purple); scale bar 50 µm. **f**) Microscopy images of lungs sections of mice as in **a** stained with DNA-binding dye (DAPI) blue; Ym1 (yellow) and Ym2 (red). Scale bar; 50 µm. Images are representative of n=5 mice per group. Quantification of antibody positive staining intensity from stained sections. Ym1 and Ym2 intensity in lung parenchyma areas and Ym2 intensity in airway epithelial cells normalised to length of airway basement membrane. **g**) Microscopy images of immunofluorescent staining for Ym1 (yellow) and Ym2 (red) in lung sections for mice as in **f**. Images show areas where co-staining in airway epithelial or parenchyma cells is evident. Triangles superimposed onto images show $Ym1^{+}Ym2^{-}$ cells (yellow), $Ym1^{-}Ym2^{+}$ cells (red) or $Ym1^{+}Ym2^{+}$ cells (white). Centre image scale bar, 100 µm; outer images scale bar, 50 µm. Datapoints depict individual animals with bars representing mean and sem (**a, b & d**) or distribution of all datapoints (at least 5 airways per mouse) with median (solid line) and 1st and 3rd quartiles represented by the lower and upper dotted lines respectively (**f**). Data are representative of 2 experiments. Data was analysed by ANOVA with Tukey's multiple comparison test with significance level showing comparisons between either PBS animals within each strain and each time point or C57BL/6 to BALB/c mice as indicated on the graph. NS not significant; *P<0.05, ** P<0.01, ***P<0.001, ****P<0.0001

Allergen-induced immune pathways are fundamentally different between C57/BL6 and BALB/c mouse strains

Whilst both C57BL/6 and BALB/c mice developed neutrophilic and eosinophilic airway inflammation in response to chronic allergen administration, there was a greater magnitude of both type 2 and type 17 cytokine responses in BALB/c mice. Therefore, to more broadly characterise the differences in immune response between mouse strains, we performed differential gene expression analysis of whole lung RNA after 8 weeks of allergen or PBS administration using the NanoString nCounter Myeloid Innate Immunity Panel (NanoString, Amersham, UK). Principle component analysis (PCA) demonstrated a clear separation in gene signatures not only from exposure to DRA versus PBS, Principle Component (PC) 1, but also mouse strain, explained by PC2 (**Fig 4a**). Investigation of the genes that were significantly altered in the DRA model showed that numerous genes are induced (e.g. type 2 effector molecules

Retnla and *Arg1*) or inhibited (e.g. basement membrane collagens, *Col4a1*, *Col4a1*) to an equivalent degree in both strains (**Sup Fig 2a**). However, hierarchical clustering also separated a considerable number of genes that were regulated in the same way across the strains, but to a much higher degree in one mouse strain over the other (**Fig 4b**) or expression of genes that were fundamentally different between strains (**Sup Fig 2b**). As predicted from the allergic cytokine responses and immune cell infiltration (**Fig 1 & 2**), type 2 related genes such as *Il13*, *Fcer2a*, *Csf2, Ccl2*, *Ccl11* were more highly upregulated in allergic BALB/c compared to C57BL/6 mice (**Fig 4b**). However, interestingly factors known to play an important role in leukocyte adhesion (*Itgb2*, *Itgb7*, *Selplg*) were upregulated in allergic C57BL/6 mice but not BALB/c mice (**Fig 4b**), despite an apparent slower rate of inflammatory cell accumulation in C57BL/6 compared to BALB/c mice (**Fig 1**).

Analysis of common properties within a signalling pathway (canonical pathway) showed enrichment of various pathways in C57BL/6 compared to BALB/c mice (**Fig 4c**). Whilst pathways including 'IL-4 signalling' and 'airway pathology in COPD' were significantly different across mouse strains, examining the genes of each pathway shows no clear direction of regulation, as denoted by the z-score (**Fig 4c**). Interestingly, both 'OX40 signalling' and 'PD-1, PD-L1 signalling', pathways involved in maintenance and regulation of T cell responses, were downregulated in allergic C57BL/6 compared to BALB/c mice (**Fig 4d**), possibly explaining reduced cytokine production in C57BL/6 mice (**Fig 2**). In addition, LXR/RXR activation, which maintains cholesterol homeostasis but is also known to be anti-fibrotic and anti-inflammatory[42], was downregulated in C57BL/6 mice (**Fig 4c and 4d**).

Overall, analysis of gene regulation at chronic allergic inflammatory time points suggested clear differences in gene signatures between mouse strains that may explain reduced immune responses in C57BL/6 compared to BALB/c mice. Analysis of canonical pathways demonstrated a reduction in pathways involved in DC-T cell stimulation in C57BL/6 compared to BALB/c mice, but a potential failure to activate LX/RX receptors known to regulate inflammation and fibrosis.

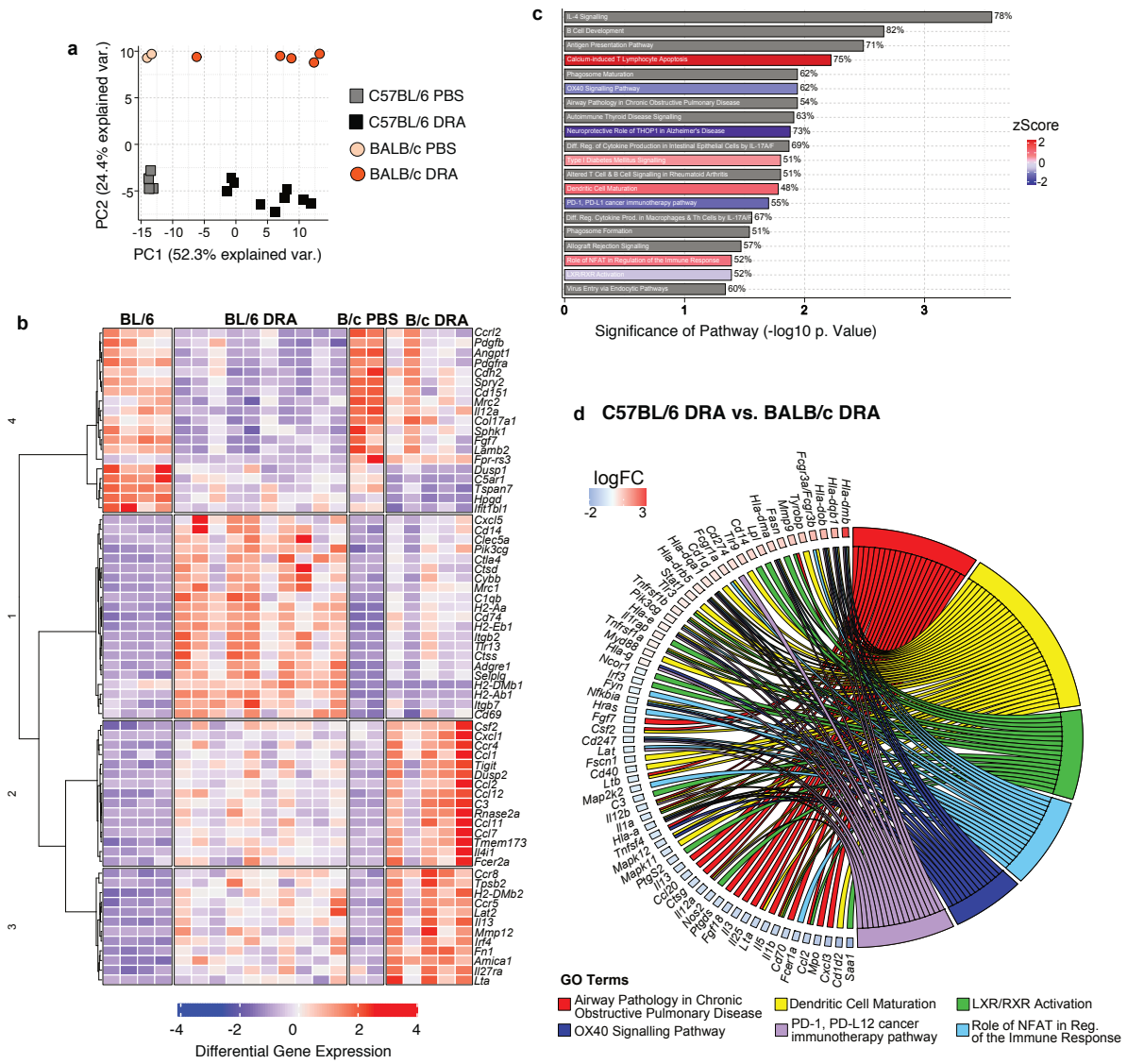

Fig 4: C57BL/6 and BALB/c allergic mice have fundamental differences in immune gene signatures

Whole lung RNA from C57BL/6 and BALB/c mice administered with either PBS or DRA for 8 weeks were analysed using NanoString Myeloid Panel v2. **a**) PCA of expressed genes from C57BL/6 and BALB/c. **b**) Unsupervised, hierarchically clustered heatmap of genes that were significantly regulated in C57BL/6 and BALB/c allergic compared to PBS mice, but also differential regulated between the treated strains. **c**) Differentially expressed genes were visualised with Ingenuity Pathway Analysis tool and top 20 canonical pathways shown for C57BL/6 versus BALB/c mice. Red or blue indicates pathways upregulated or downregulated (respectively) in C57BL/6 compared BALB/c allergic mice. Grey indicates pathways that are significantly regulated but in a particular direction. Percentage at end of the bar gives the percent coverage of molecules measured within each pathway. **d**) Chord diagram shows specific genes up or down regulated (colour indicating log fold change) within Go Term that were found to be significantly regulated in C57BL/6 allergic mice compared to BALB/c allergic mice.

Airway remodelling develops in both C57BL/6 and BALB/c mice despite different allergic inflammation dynamics and immune signatures

The relationship between inflammation and airway remodelling in asthma is still controversial (reviewed in [43-45]). Some features of remodelling may occur in parallel or even prior to excessive inflammation[20-22] although difficult to test in the clinical setting. Considering different immune cell dynamics between BALB/c and C57BL/6 mice (**Fig 1-4**), we sought to determine whether features of airway remodelling also varied between mouse strains.

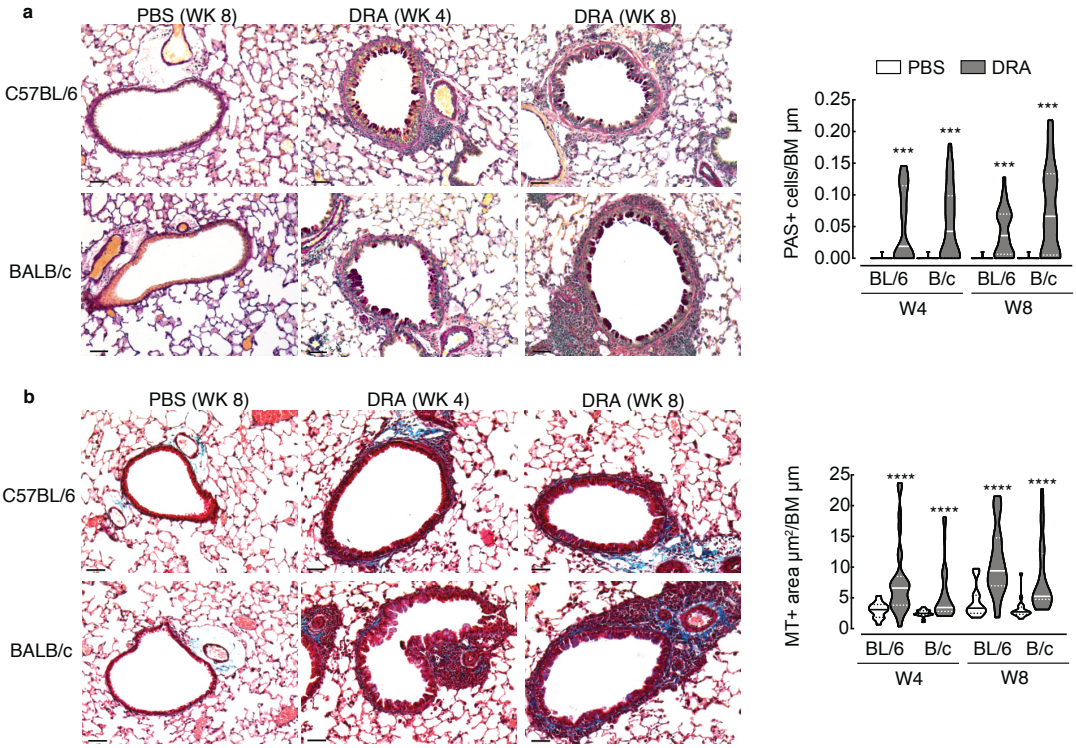

Figure 5: Goblet cell numbers and total collagen increases around the airways following exposure to DRA allergens.

C57BL/6 or BALB/c mice were intranasally administered PBS or DRA twice a week up to 8 weeks, and lungs collected for histological analysis 5 days after the last PBS or DRA at weeks 4 and 8. **a**) Microscopy images of lung sections stained for PAS. Airways show PAS$^+$ cells (purple) within the epithelium. Graph shows quantification of numbers of PAS$^+$ cells per length of basement membrane. **b**) Microscopy images of lung sections stained for Masson's trichrome from C57BL/6 or BALB/c mice. Airways show accumulation of collagen (blue) below the basement membrane. Graph shows quantification of the area of Masson's trichrome positive staining around the airways normalised to basement membrane length. All images are representative of n=5 mice; scale bar equals 50 µm. Violin plots depict distribution of all datapoints (at least 5 airways per mouse) with median (solid line) and 1st and 3rd quartiles represented by the lower and upper dotted lines respectively. Data are representative of 2 experiments. Data was analysed by ANOVA with Tukey's multiple comparison test and significance level shown relative to PBS animals within each strain and each time point. ***P<0.001, ****P<0.0001.

Goblet cell hyperplasia is a key feature of remodelling in asthma and contributes to excessive airway mucus secretion. Equivalent increases in periodic acid schiff (PAS) positive cells, indicative of goblet cells, were observed in both C57BL/6 and BALB/c mice at weeks 4 and 8 (**Fig 5a**). Airway remodelling in asthmatic patients is also characterized by thickening of the basement membrane and deposition of sub-epithelial extracellular matrix proteins. Following DRA allergen exposure, increased collagen deposition, measured by Masson's Trichrome stain, was also evident around the airways of both mouse strains (**Fig 5b**). Specific immunostaining for components of the ECM (**Fig 6a-c**) previously described to be regulated in asthma [46-49], supported increases in total airway collagen following allergen exposure (**Fig 5b**). However, fundamental differences in collagen expression between mouse strains were also evident (**Fig 6a & b**). Basement membrane protein collagen IV was highly expressed in the steady-state around the airways and alveoli of BALB/c mice compared to C57BL/6 (**Fig 6a**). Upon allergen administration, collagen IV expression decreased over time in BALB/c mice, whereas levels transiently increased in C57BL/6 mice. Additionally, a greater and more rapid increase in airway collagen I in allergic C57BL/6 compared to BALB/c mice was observed (**Fig 6a**) and similarly, accumulation of airway collagen III was significantly increased only in allergic C57BL/6 mice (**Fig 6b**). In contrast, expression of a major glycosaminoglycan component of the ECM, hyaluronan (HA), was increased in response to allergen exposure independently of mouse strain (**Fig 6b**). Changes to collagen composition around the airways of allergic mice was accompanied by an increase in the number of vimentin positive cells (**Fig 6c**), potentially indicating an increase in matrix-secreting fibroblasts[50]. Additionally, airway muscle mass was also examined and revealed increases in allergic mice regardless of mouse strain (**Fig 6c**). Overall, administration of a multi-allergen cocktail to mice, led to type 2 and type 17 inflammatory responses, characterized by eosinophil and neutrophil accumulation in the airways. However, despite greater and more rapid inflammatory cell accumulation in BALB/c compared to C57BL/6 mice, features of remodelling like goblet cell hyperplasia, smooth muscle mass and ECM deposition were evident in both strains, suggesting that inflammatory cell dynamics are not the key determinant of airway remodelling.

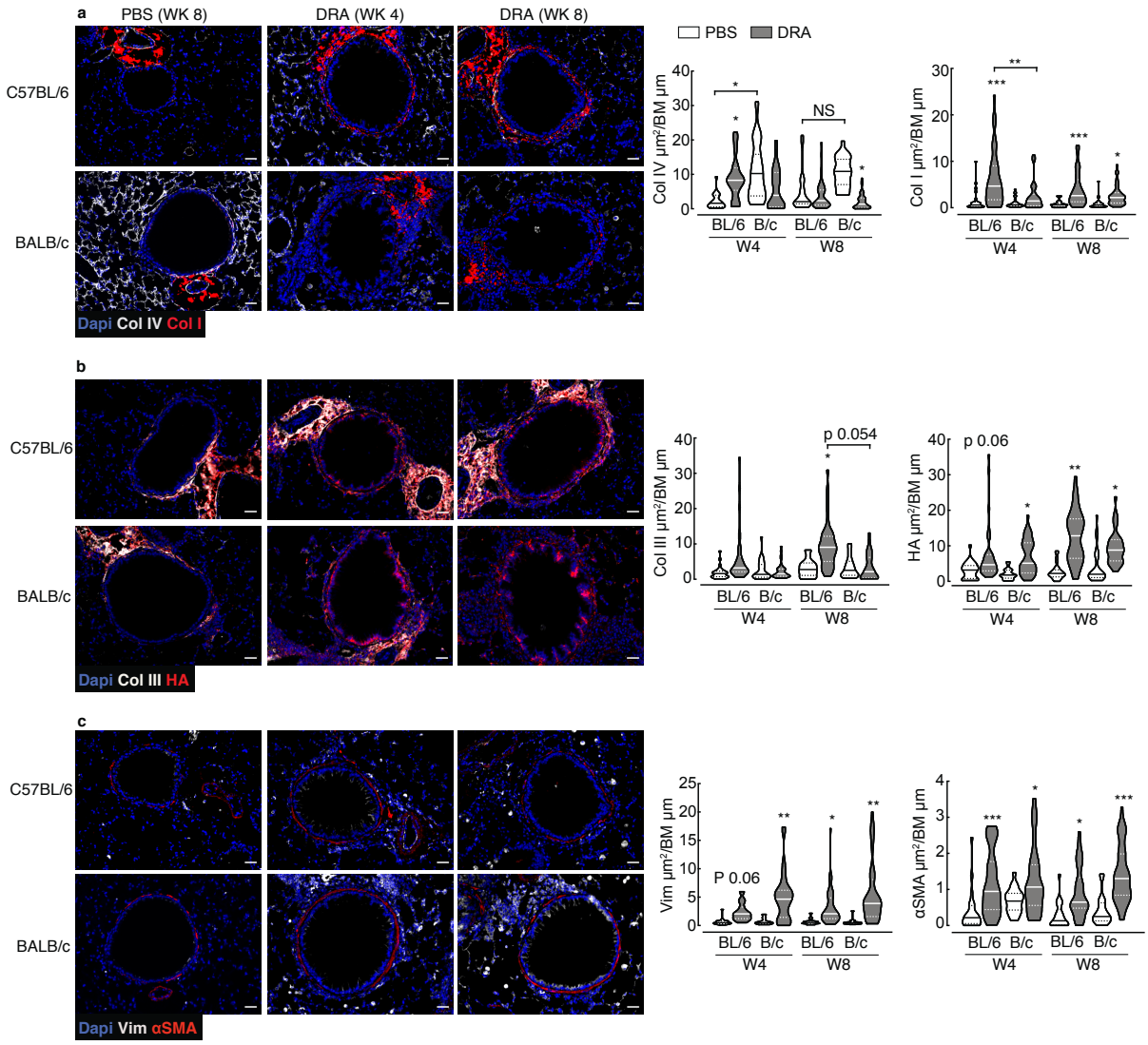

Figure 6: Changes to the ECM and muscle mass around the airway occur following exposure to DRA allergens.

C57BL/6 or BALB/c mice were intranasally administered PBS or DRA twice a week up to 8 weeks, and lungs collected for immuno-staining 5 days after the last PBS or DRA at weeks 4 and 8. **a-c**) Microscopy images of lung sections from C57BL/6 or BALB/c mice stained with DNA-binding dye (DAPI) blue; (**a**) Col IV white; Col I red; (**b**) Col III, white; hyaluronan (HA) binding protein, red; (**c**) vimentin (Vim) white; alpha smooth muscle actin (αSMA) red. Scale bar, 30 µm. Images are representative of n=5 mice. Antibody positive staining area was quantified around the airway and normalised to basement membrane length and values are depicted in graphs **a-c**. Violin plots depict distribution of all datapoints (at least 5 airways per mouse) with median (solid line) and 1st and 3rd quartiles represented by the lower and upper dotted lines respectively. Data are representative of 2 experiments. Data was analysed by ANOVA with Tukey's multiple comparison test and significance level showing comparisons between either PBS animals within each strain and each time point or C57BL/6 to BALB/c mice as indicated on the graph. *P<0.05, ** P<0.01, ***P<0.001.

Discussion

IL-17 and neutrophilia are often associated with severe asthma[10]. Despite this, models of allergic airway inflammation still largely focus on studying the regulation of allergen induced type 2 immune responses, utilising BALB/c mice that generally show a strongly skewed type 2 inflammatory response[27]. Here, we utilised a model of allergic airway inflammation whereby neutrophilia and IL-17 are dominant features, with inflammation resistant to steroid intervention[29] and AHR unaffected by neutralisation of IL-5 or IL-13 cytokines[28]. As expected BALB/c mice developed rapid and prominent airway inflammation that was skewed toward type 2 responses, but also greater IL-17 production, particularly by γδ T cells. Whilst C57BL/6 mice still responded to allergens, Th2 and IL-17A responses developed at a slower rate compared to BALB/c mice. Delayed type 2 cytokine expression is potentially explained by an early but transient spike in IFNγ expression only observed in C57BL/6 mice. Interestingly, increased IL-17A expression in C57BL/6 mice between weeks 4 and 8 coincided with a reduction in IFNγ levels in allergic mice, which we have shown previously to be an important factor that allows the development of a pulmonary type 2 immue response[51]. Additionally, IL-10 derived from T cells has been shown to signal via alveolar macrophages leading to suppression of IFNγ-induced airway epithelial disruption[52]. No difference in expression of *Il10* between strains at chronic time points was observed after DRA administration in our study. However, temporal changes in IL-10 in C57BL/6 mice may contribute to suppression of IFNγ alongside IL-17A.

IL-13 production is known to be higher in BALB/c versus C57BL/6 mice[27], as also shown here, and is thought to account for increased AHR observed in BALB/c compared to the relatively hypo-responsive C57BL/6 mice[23,53]. In fact, type 2 cytokine producing cells, rather than eosinophilic inflammation, appear to be key for the maintenance of AHR in models of type 2 airway inflammation[54,24]. In addition to enhanced type 2 cytokine production, pathway analysis suggested a reduced capacity (in C57BL/6 mice) for antigen-presenting cell (APC) mediated activation of T cells via costimulatory molecules PD-1/PDL-1 and OX40/OX40L, despite enhanced 'DC maturation' pathways from NanoString analysis in these mice. Different DC subsets can dictate the allergic immune response and targeting either DC activation or molecules involved in antigen presentation may be a fruitful approach to therapeutically target allergic asthma, and specifically different immune phenotypes of

disease[55,56]. PDL1 is known to enhance AHR and Th2 cytokine production in allergic mice[57]. Thereby a reduction in PD1-PDL1 signalling, alongside reduced OX40 signalling may explain the reduced Th2 response in C57BL/6 mice compared to BALB/c. Future research identifying specific dendritic cell phenotypes in both strains during AAI could prove useful for understanding pathways to target AHR and inflammation in asthma.

In this model of Th1/Th17 allergic airway inflammation, both BALB/c and C57BL/6 mice developed a similar degree of airway remodelling in response to allergen exposure. However, our study reveals intriguing differences in ECM composition between mouse strains, not only in response to allergens but also in the steady state. One could anticipate that changes in collagen composition, particularly centred around the ratios of collagen I and III, could profoundly alter lung function and along with varied immune responses, may contribute to well reported differences in AHR measurement between mouse strains[23,53]. Both collagen I and III play major roles in the structural integrity of tissues and are often co-expressed within the tissue, with Col I contributing to tensile strength, whilst Col III allows tissue flexibility[58]. Collagen III can modulate scar formation[59] and during early active fibrosis levels of Col III significantly increase[60,61]. However, an increased ratio between type I and type III collagen occurs in infants diagnosed with chronic lung disease proceeding respiratory distress syndrome[60]. Additionally, a lack of collagen III can disturb the development of collagen fibril formation resulting in functional failure of the organ[62,63]. Here, allergic BALB/c mice appeared to have preferential increase in collagen I around the airways, with no significant changes to collagen III, although we cannot rule out expression of collagen III at time points earlier than week 4. A failure to induce collagen III during remodelling processes may in fact perturb lung function, perhaps contributing to increases in AHR often observed in BALB/c mice in response to allergen challenge[23,27,53]. Differential dynamics in col IV expression between mouse strains is also intriguing, as Col IV is crucial for barrier formation anchoring airway epithelial cells. The rapid loss of Col IV in BALB/c mice may relate to a significant increased vimentin-positive cells around the airway at week 4, and potentially enhanced epithelial mesenchymal transition leading to a more rapid remodelling response in BALB/c versus C57BL/6. Although both mouse strains feature a similar magnitude of allergen-induced remodelling, further analysis of the early dynamics, pre-week 4, and mechanisms leading to changes in

the ECM in these two mouse strains may reveal important features of tissue remodelling in disease.

Remodelling is typically examined as a change in epithelial goblet hyperplasia, increased muscle mass and total collagen, but here our study in genetically distinct mouse strains, highlights that the term remodelling is much more complicated. Just as inflammation varies greatly between asthmatic cohorts, airway remodelling too may be considered an “umbrella” term, whereby different pathways are likely to be more or less important in different asthma phenotypes. A greater understanding of how ECM composition changes can alter lung mechanics/function, but also how the differing ECM components can regulate immune cell recruitment and activation, will help us to understand the development of lung diseases like asthma and whether approaches to target remodelling will prove useful in treating such chronic inflammatory diseases. Furthermore, it is interesting to speculate that different genetic strains of mice, rather than using different allergens of timings of allergen exposure, could prove more useful for modelling different trajectories of allergic asthma in people.

Methods

Animals and Ethics

Wild-type (BALB/c or C57BL/6J) mice were obtained from a commercial supplier (Envigo, Hillcrest, UK). Experimental mice, all female, were between 7-10 weeks old at the start of the experiment and were housed in individually ventilated cages maintained in groups of 5 animals in specific pathogen-free facilities at the University of Manchester. Mice were not randomised in cages, but each cage was randomly assigned to a treatment group. Sample size was calculated on the basis of the number of animals needed for detection of a 25% change in Masson's trichrome positive area around the airway in PBS versus allergic mice, with a P value of <0.05, based on pilot experiments carried out with 3 mice per group. All animal experiments were performed in accordance with the UK Animals (Scientific Procedures) Act of 1986 under a Project License (70/8548) granted by the UK Home Office and approved by the University of Manchester Animal Welfare and Ethical Review Body. Euthanasia was performed by asphyxiation in a rising concentration of carbon dioxide.

Model of allergic airway inflammation

Allergic airway inflammation was induced in mice in a similar manner as has been described previously[28]. Allergen DRA cocktail comprising of 5 µg House Dust Mite (*Dermatophagoides pteronyssinus,* 5450 EU, 69.23 mg per vial), 50 µg Ragweed (*Ambrosia artemisifolia*), 5 µg *Aspergillus fumigatus* (Greer Laboratories) extracts were freshly prepared prior to each inoculation. Mice were briefly anaesthetised via inhalation of isoflurane, and 20 µL of DRA cocktail or PBS were given via intranasal inoculation twice weekly for up to 8 weeks. Mice were rested for 5 days prior to performing BAL and collecting lung tissue.

Isolation of cells from the BAL and lung tissue

Following exsanguination, BAL cells were obtained through cannulation of the trachea and washing the lungs with 0.4 mL PBS containing 0.25 % BSA (four washes). Lungs were processed as previously described[41]. Briefly, a right lobe was removed and minced in 1 mL of HBSS buffer containing 0.4 U/mL Liberase TL (Sigma) and 80 U/mL DNase type I (Life Tech) for 25 min in a 37ºC shaking incubator. Digestion was stopped with 2 % FBS (Gibco) and 2 mM EDTA prior to passing the suspension through a 70

µm cell strainer (Greiner). Red blood cells were lysed (Sigma) and total live BAL and lung cell counts assessed with Viastain AOPI (Nexcelom, Bioscience) using a Cellometer Auto2000 automated cell counter (Nexcelom, Bioscience).

Flow Cytometry

Equal cell numbers of each lung and BAL sample were stained for flow cytometry. Cells were washed with ice-cold PBS and stained with Live/Dead Aqua or Blue (life Tech) for 10 min at room temperature. All samples were then incubated with Fc block (5 µg/mL CD16/CD32 and 0.1% mouse serum in FACs buffer (PBS containing 0.5% BSA and 2 mM EDTA)) for 20 min before staining for specific surface markers with fluorescence-conjugated antibodies for 25 min at 4ºC (**Table 1**) Following surface staining, cells were fixed with ICC fix (Biolegend) and stored at 4ºC until intracellular staining was performed or cells were acquired. For intracellular cytokine staining, cells were stimulated for 4h at 37ºC with PMA (phorbol myristate acetate; 0.5 µg/mL) and ionomycin (1 µg/mL) and for 3 h at 37ºC with Brefaldin A (10 µg/mL; Biolegend). Cell surfaces were stained and cells fixed as described above. All cells were permeabilized (eBioscience) then stained with antibodies for intracellular cytokines (**Table 1**). Eosinophils were identified as F4/80^{+} CD11c^{-} CD11b^{+} SigF^{+} CD64^{-} and neutrophils identified as Ly6G^{+} CD11b^{+} CD11c^{-} CD64^{+}. All samples were acquired with a FACS Canto II or 5 laser Fortessa with BD FACS Diva software and analysed with FlowJo software (versions 9 and 10; Treestar).

RNA extraction and qRT-PCR

One right lung lobe was stored in RNAlater (Life Tech) prior to homogenization in Qiazol reagent (Qiagen). RNA was prepared according to manufacturer's instructions and stored at -70 ºC. Reverse transcription of 0.2-0.5 µg total RNA was performed using 50 U Tetro reverse transcriptase (Bioline), 40 mM dNTPs (Promega), 0.5 µg primer for cDNA synthesis (Sigma) and RNasin inhibitor (Promega). The transcripts for genes of interest were measured by real-time PCR with a Lightcycler 480 II system (Roche) and a Brilliant III SYBR Green Master mix (Agilent) with specific primer pairs (**Table 2**). mRNA amplification was analysed by second derivative maximum algorithm (LightCycler 480 Sw 1.5; Roche) and expression of the gene of interest was

normalised to the geometric mean of three housekeeping genes *Rn45s*, *Rpl13a*, *Gapdh* (**Table 2**).

Table 1: Antibodies used for flow cytometry analysis

Antigen	Antibody Clone	Isotype	Source
Ly6G	1A8	Rat IgG2a κ	Biolegend
CD11b	M1/70	Rat IgG2b κ	Biolegend
CD11c	N418	Armenian Hamster IgG	Biolegend
F4/80	BM8	Rat IgG2a κ	Biolegend
CD64	X54-5/7.1	Mouse IgG1 κ	Biolegend
SiglecF	E50-2440	Rat IgG2a κ	BD Biosciences
I-A/I-E	M5/144.15.2	Rat IgG2b κ	Biolegend
TCRβ	H57-597	Armenian Hamster IgG	eBioscience
TCRɣδ	GL3	Armenian Hamster IgG	Biolegend
CD4	GK1.5	Rat IgG2b κ	Biolegend
CD8	53-6.7	Rat IgG2a κ	Biolegend
IL-4	11b11	Rat IgG1 κ	Biolegend
IL-13	eBio13A	Rat IgG1 κ	eBioscience
IL-17a	TC11-18H10.1	Rat IgG1 κ	Biolegend
IFNɣ	XMG1.2	Rat IgG1 κ	Biolegend

Table 2: Sequences of primers for measurement of mRNA expression via qRT-PCR

Gene	Forward Primer	Reverse Primer
Il4	CCTGCTCTTCTTTCTCGAATG	CACATCCATCTCCGTGCAT
Il13	CCTCTGACCCTTAAGGAGCTTAT	CGTTGCACAGGGGAGTCT
Il5	ACATTGACCGCCAAAAAGAG	CACCATGGAGCAGCTCAG
Il17a	GCTCCAGAAGGCCCTCAGACT	CCAGCTTTCCCTCCGCATTGA
Ifng	GGAGGAACTGGCAAAAGGAT	TTCAAGACTTCAAAGAGTCTGAGG
Chil1	CCAGCCAGGCAGAGAGAAAC	GCCACCTTTCCTGCTGACA
Chil3	TCTGGTGAAGGAAATGCGTAAA	GCAGCCTTGGAATGTCTTTCTC
Chil4	TCTGGTGCAGGAAATGCGTAAA	GCAGCCTTGGAATGTGGTTCAAAG
Rn45s	GTAACCCGTTGAACCCCATT	CCATCCAATCGGTAGTAGCG
Rpl13a	CATGAGGTCGGGTGGAAGTA	GCCTGTTTCCGTAACCTCAA
Gapdh	ATGACATCAAGAAGGTGGTG	CATACCAGGAAATGAGCTTG

Transcriptome profile and associated analysis

Quality of RNA extracted from lung tissue, as described above, was assessed with Agilent 2200 TapeStation system prior to downstream analyses, samples with an RIN value of <5.5 were excluded. RNA concentration was determined using Qubit TM RNA BR Assay Kit (Thermofisher) and 100 ng RNA (per sample) run on a Nanotstring nCounter R FLEC system using the Myeloid Innate Immunity v2 panel (XT-CSO-MMII2-12). Note, the probes in this panel do not distinguish between *Chil3* and *Chil4*. Raw counts were uploaded onto nSolver version 4.0 using default settings. Non-normalised counts were exported, and subsequent analyses performed in R (version 3.6.3) using RStudio Version 1.2.5033 (2009-2019 RStudio, Inc). Positive controls were analysed to ensure there was clear resolution at variable expression levels and negative controls were used to set a minimum detection threshold which was then applied to all samples. Data were normalised with EdgeR using the Upper Quartile method and differential expression of genes calculated via linear modelling accounting for sample quality weights with Empirical Bayes smoothing using the limma-voom R packages[64]. All genes expressed above the background threshold were used for principal component analysis (PCA). Genes with an absolute fold change of greater than 0.5 and a significance value of under 0.05 after correction for multiple comparisons using the Benjamini-Yekeuteli method were defined as “differentially expressed” and taken forward for further analysis. Heatmaps were then generated from scaled normalized counts of DE genes using the ComplexHeatmaps R package. The networks and functional analyses of DE genes were generated with Ingenuity Pathway Analyser (IPA; QIAGEN Inc., https://www.qiagenbio-informatics.com/products/ingenuity-pathway-analysis). Within the IPA software no tissue filtering was used and the user dataset was defined as the reference. Pathway data were then imported into R for visualisation using the ggplot package.

Generating Anti-Ym2 and determining antibody specificity

Anti-Ym2 specific antibodies were generated by Cambridge Research Biochemicals. The 9 amino acid sequence at the N-terminal (CKASYRGEL) were used as the immunogen as it has almost no homology to the Ym1 sequence. Bacterial optimised expression plasmids for Ym1 and Ym2 were purchased from (Genscript). Plasmids were then transfected into competent *E. Coli* (BL21) using heat shock followed antibiotic selection against Ampicillin (Amp; 25 mg/mL) and Chloramphenicol (Chl; 34

mg/mL). To generate recombinant protein a small scraping of the stock sample was expanded in LB media including antibiotics until optical density reached between 0.6-1.0 at which point IPTG (0.1 M) was added to the cultures. The OD was kept under 1.0 by diluting the culture with fresh media as required and left overnight. Thereafter bacteria were pelleted and resuspended in loading buffer containing DTT (200 mM; Thermo Fischer Scientific).

Western Blotting

Lysed Ym1 or Ym2 transfected *E.coli* cells and murine BAL were denatured in the presence of DTT (200mM; Thermo Fischer Scientific) for 5 mins at 95 ºC. Each sample (2-10 µL) or protein ladder (Seeblue, Thermo Fischer Scientific) was separated on Bis-Tris 4-12% gradient gel with MES buffer (Thermo Fischer Scientific) before transfer onto a PVDF membrane. The membrane was washed in distilled water followed by incubation in blocking buffer (5% BSA in PBST (0.05% Tween-20 in PBS)) for 60 mins at room temperature on a rocking platform. Primary antibodies were used at 1:500 (rabbit anti-mouse Ym2, polyclonal (custom made) or goat anti-mouse Ym1 polyclonal (R&D)) and incubated at room temperature over-night on a rocking platform. The membrane was then washed in PBST followed by secondary antibody detection (1:1000 anti-Rabbit IgG Cy3 and Streptavidin-Cy3, Thermo Fischer Scientific) for one hour at room temperature. Membranes were imaging using a Gel Doc (Azure Biosystems, Cambridge Bioscience).

Histology and Immunostaining

The left lung lobe was fixed perfused with 10 % neutral buffered formalin (Sigma) and was incubated overnight before being transferred to 70 % ethanol. Lungs were processed and embedded in paraffin, then sectioned (5 µm) and stained with Masson's trichrome (MT) or periodic acid schiff (PAS) stains using standard protocols. Images were captured with a Leica microscope with digital DMC2900 camera. For immunostaining with antibodies, lung sections were deparaffinised and heat-mediated antigen retrieval performed using Tris-EDTA buffer (10 mM Tris Base, 1 mM EDTA, 0.05 % Tween-20 pH 8.0; incubation 20 min 95ºC). Non-specific protein was blocked with 2% normal donkey serum in PBS containing 0.05 % Tween-20 and 1 % BSA. If a biotin labelled antibody or probe was used, avidin biotin block (Thermo) was performed prior to an overnight incubation at 4ºC with primary antibodies (Table 3). Sections were

washed in PBS before incubation with secondary antibodies (**Table 3**) for 1 hr at room temperature followed by mounting with DAPI containing fluoromount (Southern biotech).

Table 3: Antibodies used for immune-histological analysis

Antigen	Antibody Clone	Dilution	Source
Ym1	Goat polyclonal - Biotinylated	1:100	R&D – BAF2446
Ym2	Rabbit polyclonal	1:1000	Home-made
Collagen I	Goat polyclonal	1:200	Cambridge Bioscience – 1310-01
Collagen III (N-terminal)	Rabbit polyclonal	1:300	Proteintech – 22734-1-AP
Collagen IV alpha I	Rabbit polyclonal	1:200	Novus Biologicals – NB120-6586
Hyaluronan binding protein	Biotinylated	1:100	Merck Millipore - 385911
α-Smooth muscle actin	Goat polyclonal	1:200	Novus Biologicals – NB-300-978
Vimentin	Rabbit polyclonal	1:200	Abcam – ab45939
BRP-39	Rabbit Polyclonal	1:100	Biorbyt – orb10365
-	Streptavidin 557	1:800	R&D – NL999
-	Streptavidin 637	1:400	R&D – NL998
-	Donkey anti-rabbit IgG 557	1:200	R&D – NL004
-	Donkey anti-rabbit IgG 637	1:200	R&D – NL005
-	Donkey anti-goat IgG 557	1:200	R&D – NL001
-	Donkey anti-goat IgG 637	1:200	R&D – NL002

Images were captured with an EVOS FL imaging system (Thermo). Analysis of images was performed using ImageJ software (version 2.09.0-rc69/1.52p) on sections where sample identification was blinded for the investigator and airways analysed had to be intact and fit within a single microscope field of view 480 µm x 360 µm. Goblet cells were visualised on PAS-stained sections and numbers of PAS+ cells counted per airway and normalised to the length the airway basement membrane. Total collagen area was calculated by measuring the area of Masson's trichrome positive stain (blue) around the airway and values were normalised to basement membrane length. For calculation of collagen, hyaluronan, vimentin and αSMA area, background autofluorescence was subtracted from all images based on pixel intensities of sections stained with secondary antibodies only. A region of interest was drawn parallel to the

airway basement membrane at a distance of 50 μm. A threshold was applied to all images to incorporate positively stained pixels and area of positively stained pixels within the region of interest calculated and normalised to the length of the basement membrane. All areas of the airway that contained a blood vessel was excluded from analysis to ensure measurements specifically related to airways and not vasculature. For all image analysis, between 5-15 airways were measured per mouse.

Quantification of Ym1 and BRP-39

The levels of Ym1 and BRP-39 in the serum and BAL were measured by sandwich ELISA, with DuoSet ELISA kits (R&D) as per manufacturers recommendation.

Statistical analysis

Statistical analysis was performed using JMP Pro 12.2.0 for Mac OS X (SAS Institute Inc.). Normal distribution of data was determined by optical examination of residuals, and each group was tested for unequal variances using Welch's test. Differences between groups were determined by analysis of variance (ANOVA) followed by a Tukey-Kramer HSD multiple comparison test or unpaired two-tailed Student's t-test as indicated in figure legends. In some data sets, data were log transformed to achieve normal distribution. Differences were considered statistically significant for *P* values of less than 0.05.

Acknowledgments

This work was supported by the Medical Research Foundation UK jointly with Asthma UK (MRFAUK-2015-302 to TES), the Medical Research Council UK (MR/P02615X/1 to DR and MR/K01207X/1 to JEA) and the Wellcome Trust (106898/A/15/Z to JEA). The authors would like to thank Brian Chan for his technical support, Alistair Chenery and Anthony Day for *E. coli* expressing recombinant Ym1 and Ym2 and Conor Finlay for critical reading of the manuscript. We also thank the Flow Cytometry, Histology and Biological Services core facilities at the University of Manchester.

Conflict of Interest

The authors declare no competing financial interests.

Author Contributions

James E Parkinson: Data curation; investigation; methodology; formal analysis; writing – original draft; Writing – reviewing and editing. **Stella Pearson**: investigation; methodology. **Dominik Rückerl:** investigation; writing – reviewing and editing. **Judith E Allen**: Funding acquisition; investigation; writing – reviewing and editing. **Tara E Sutherland**: Conceptualisation; Investigation; methodology; project administration; supervision; funding acquisition; writing – original draft; writing – review and editing.

References

1 The Global Asthma Report, Auckland, New Zealand. *New Zealand* 2018; 1–92.

2 Custovic A, Henderson J, Simpson A. Does understanding endotypes translate to better asthma management options for all? *J Allergy Clin Immunol* 2019; **144**: 25–33.

3 Pavord ID, Beasley R, Agusti A, Anderson GP, Bel E, Brusselle G *et al.* After asthma: redefining airways diseases. *Lancet* 2018; **391**: 350–400.

4 Kuruvilla ME, Lee FE-H, Lee GB. Understanding Asthma Phenotypes, Endotypes, and Mechanisms of Disease. *Clin Rev Allergy Immunol* 2019; **56**: 219–233.

5 McGregor MC, Krings JG, Nair P, Castro M. Role of Biologics in Asthma. *Am J Respir Crit Care Med* 2019; **199**: 433–445.

6 Hansbro PM, Kaiko GE, Foster PS. Cytokine/anti-cytokine therapy - novel treatments for asthma? *British Journal of Pharmacology* 2011; **163**: 81–95.

7 Pavord ID, Korn S, Howarth P, Bleecker ER, Buhl R, Keene ON *et al.* Mepolizumab for severe eosinophilic asthma (DREAM): a multicentre, double-blind, placebo-controlled trial. *Lancet* 2012; **380**: 651–659.

8 Haldar P, Brightling CE, Singapuri A, Hargadon B, Gupta S, Monteiro W *et al.* Outcomes after cessation of mepolizumab therapy in severe eosinophilic asthma: a 12-month follow-up analysis. *J Allergy Clin Immunol* 2014; **133**: 921–923.

9 Busse WW, Holgate S, Kerwin E, Chon Y, Feng J, Lin J *et al.* Randomized, double-blind, placebo-controlled study of brodalumab, a human anti-IL-17 receptor monoclonal antibody, in moderate to severe asthma. *Am J Respir Crit Care Med* 2013; **188**: 1294–1302.

10 Lindén A, Dahlén B. Interleukin-17 cytokine signalling in patients with asthma. *European Respiratory Journal* 2014; **44**: 1319–1331.

11 Andersson CK, Adams A, Nagakumar P, Bossley C, Gupta A, De Vries D *et al.* Intraepithelial neutrophils in pediatric severe asthma are associated with better lung function. *J Allergy Clin Immunol* 2017; **139**: 1819–1829.e11.

12 Patel DF, Peiró T, Bruno N, Vuononvirta J, Akthar S, Puttur F *et al.* Neutrophils restrain allergic airway inflammation by limiting ILC2 function and monocyte-dendritic cell antigen presentation. *Sci Immunol* 2019; **4**: eaax7006.

13 Beers MF, Morrisey EE. The three R's of lung health and disease: repair, remodeling, and regeneration. *J Clin Invest* 2011; **121**: 2065–2073.

14 Hansbro PM, Kim RY, Starkey MR, Donovan C, Dua K, Mayall JR *et al.* Mechanisms and treatments for severe, steroid-resistant allergic airway disease and asthma. *Immunol Rev* 2017; **278**: 41–62.

15 Hoshino M, Takahashi M, Takai Y, Sim J, Aoike N. Inhaled corticosteroids decrease vascularity of the bronchial mucosa in patients with asthma. *Clin Exp Allergy* 2001; **31**: 722–730.

16 Laitinen A, Altraja A, Kämpe M, Linden M, Virtanen I, Laitinen LA. Tenascin is increased in airway basement membrane of asthmatics and decreased by an inhaled steroid. *Am J Respir Crit Care Med* 1997; **156**: 951–958.

17 Hoshino M, Takahashi M, Takai Y, Sim J. Inhaled corticosteroids decrease subepithelial collagen deposition by modulation of the balance between matrix metalloproteinase-9 and tissue inhibitor of metalloproteinase-1 expression in asthma. *Journal of Allergy and Clinical Immunology* 1999; **104**: 356–363.

18 Flood-Page P, Menzies-Gow A, Phipps S, Ying S, Wangoo A, Ludwig MS *et al.* Anti-IL-5 treatment reduces deposition of ECM proteins in the bronchial subepithelial basement membrane of mild atopic asthmatics. *J Clin Invest* 2003; **112**: 1029–1036.

19 Zhao J, Lloyd CM, Noble A. Th17 responses in chronic allergic airway inflammation abrogate regulatory T-cell-mediated tolerance and contribute to airway remodeling. *Mucosal Immunol* 2013; **6**: 335–346.

20 Henschen M, Stocks J, Brookes I, Frey U. New aspects of airway mechanics in pre-term infants. *Eur Respir J* 2006; **27**: 913–920.

21 Saglani S, Payne DN, Zhu J, Wang Z, Nicholson AG, Bush A *et al.* Early detection of airway wall remodeling and eosinophilic inflammation in preschool wheezers. *Am J Respir Crit Care Med* 2007; **176**: 858–864.

22 Lezmi G, Gosset P, Deschildre A, Abou-Taam R, Mahut B, Beydon N *et al.* Airway Remodeling in Preschool Children with Severe Recurrent Wheeze. *Am J Respir Crit Care Med* 2015; **192**: 164–171.

23 Van Hove CL, Maes T, Cataldo DD, Gueders MM, Palmans E, Joos GF *et al.* Comparison of acute inflammatory and chronic structural asthma-like responses between C57BL/6 and BALB/c mice. *Int Arch Allergy Immunol* 2009; **149**: 195–207.

24 Kearley J, Buckland KF, Mathie SA, Lloyd CM. Resolution of allergic inflammation and airway hyperreactivity is dependent upon disruption of the T1/ST2-IL-33 pathway. *Am J Respir Crit Care Med* 2009; **179**: 772–781.

25 Hirota JA, Ask K, Fritz D, Ellis R, Wattie J, Richards CD *et al.* Role of STAT6 and SMAD2 in a model of chronic allergen exposure: a mouse strain comparison study. *Clinical & Experimental Allergy* 2009; **39**: 147–158.

26 Shinagawa K. Mouse Model of Airway Remodeling: Strain Differences. *Am J Respir Crit Care Med* 2003; **168**: 959–967.

27 Gueders MM, Paulissen G, Crahay C, Quesada Calvo F, Hacha J, Van Hove C *et al.* Mouse models of asthma: a comparison between C57BL/6 and BALB/c strains regarding bronchial responsiveness, inflammation, and cytokine production. *Inflamm Res* 2009; **58**: 845–854.

28 Goplen N, Karim MZ, Liang Q, Gorska MM, Rozario S, Guo L *et al.* Combined sensitization of mice to extracts of dust mite, ragweed, and Aspergillus species breaks through tolerance and establishes chronic features of asthma. *J Allergy Clin Immunol* 2009; **123**: 925–32.e11.

29 Liu R, Bai J, Xu G, Xuan L, Zhang T, Meng A *et al.* Multi-allergen challenge stimulates steriod-resistant airway inflammation via NF-κB-mediated IL-8 expression. *Inflammation* 2013; **36**: 845–854.

30 Voskamp AL, Kormelink TG, van Wijk RG, Hiemstra PS, Taube C, de Jong EC *et al.* Modulating local airway immune responses to treat allergic asthma: lessons from experimental models and human studies. *Semin Immunopathol* 2020; **42**: 95–110.

31 Rosenberg HF, Druey KM. Modeling asthma: Pitfalls, promises, and the road ahead. *J Leukoc Biol* 2018; **104**: 41–48.

32 Sahu N, Morales JL, Fowell D, August A. Modeling susceptibility versus resistance in allergic airway disease reveals regulation by Tec kinase Itk. *PLoS ONE* 2010; **5**: e11348.

33 De Vooght V, Vanoirbeek JAJ, Luyts K, Haenen S, Nemery B, Hoet PHM. Choice of Mouse Strain Influences the Outcome in a Mouse Model of Chemical-Induced Asthma. *PLoS ONE* 2010; **5**: e12581–9.

34 James AJ, Reinius LE, Verhoek M, Gomes A, Kupczyk M, Hammar U *et al.* Increased YKL-40 and Chitotriosidase in Asthma and Chronic Obstructive Pulmonary Disease. *Am J Respir Crit Care Med* 2016; **193**: 131–142.

35 Liu L, Zhang X, Liu Y, Zhang L, Zheng J, Wang J *et al.* Chitinase-like protein YKL-40 correlates with inflammatory phenotypes, anti-asthma responsiveness and future exacerbations. *Respir Res* 2019; **20**: 95.

36 Ober C, Tan Z, Sun Y, Possick JD, Pan L, Nicolae R *et al.* Effect of variation in CHI3L1 on serum YKL-40 level, risk of asthma, and lung function. *N Engl J Med* 2008; **358**: 1682–1691.

37 Konradsen JR, James A, Nordlund B, Reinius LE, Söderhäll C, Melén E *et al.* The chitinase-like protein YKL-40: a possible biomarker of inflammation and airway remodeling in severe pediatric asthma. *J Allergy Clin Immunol* 2013; **132**: 328–35.e5.

38 Tong X, Wang D, Liu S, Ma Y, Li Z, Tian P *et al.* The YKL-40 protein is a potential biomarker for COPD: a meta-analysis and systematic review. *COPD* 2018; **13**: 409–418.

39 Chupp GL, Lee CG, Jarjour N, Shim YM, Holm CT, He S *et al.* A chitinase-like protein in the lung and circulation of patients with severe asthma. *N Engl J Med* 2007; **357**: 2016–2027.

40 Furuhashi K, Suda T, Nakamura Y, Inui N, Hashimoto D, Miwa S *et al.* Increased expression of YKL-40, a chitinase-like protein, in serum and lung of patients with idiopathic pulmonary fibrosis. *Respir Med* 2010; **104**: 1204–1210.

41 Sutherland TE, Ruckerl D, Logan N, Duncan S, Wynn TA, Allen JE. Ym1 induces RELMα and rescues IL-4Rα deficiency in lung repair during nematode infection. *PLoS Pathog* 2018; **14**: e1007423.

42 Smet M, Van Hoecke L, De Beuckelaer A, Vander Beken S, Naessens T, Vergote K *et al.* Cholesterol-sensing liver X receptors stimulate Th2-driven allergic eosinophilic asthma in mice. *Immun Inflamm Dis* 2016; **4**: 350–361.

43 Saglani S, Lloyd CM. Novel concepts in airway inflammation and remodelling in asthma. *European Respiratory Journal* 2015; **46**: 1796–1804.

44 Boulet L-P. Airway remodeling in asthma: update on mechanisms and therapeutic approaches. *Current Opinion in Pulmonary Medicine* 2018; **24**: 56–62.

45 Guida G, Riccio AM. Immune induction of airway remodeling. *Semin Immunol* 2019; **46**: 101346.

46 Chakir J, Shannon J, Molet S, Fukakusa M, Elias J, Laviolette M *et al.* Airway remodeling-associated mediators in moderate to severe asthma: effect of steroids on TGF-beta, IL-11, IL-17, and type I and type III collagen expression. *Journal of Allergy and Clinical Immunology* 2003; **111**: 1293–1298.

47 Benayoun L, Druilhe A, Dombret M-C, Aubier M, Pretolani M. Airway structural alterations selectively associated with severe asthma. *Am J Respir Crit Care Med* 2003; **167**: 1360–1368.

48 Johnson PRA, Burgess JK, Underwood PA, Au W, Poniris MH, Tamm M *et al.* Extracellular matrix proteins modulate asthmatic airway smooth muscle cell proliferation via an autocrine mechanism. *Journal of Allergy and Clinical Immunology* 2004; **113**: 690–696.

49 Lauer ME, Majors AK, Comhair S, Ruple LM, Matuska B, Subramanian A *et al.* Hyaluronan and Its Heavy Chain Modification in Asthma Severity and Experimental Asthma Exacerbation. *Journal of Biological Chemistry* 2015; **290**: 23124–23134.

50 Goodpaster T, Legesse-Miller A, Hameed MR, Aisner SC, Randolph-Habecker J, Coller HA. An immunohistochemical method for identifying fibroblasts in formalin-fixed, paraffin-embedded tissue. *J Histochem Cytochem* 2008; **56**: 347–358.

51 Ajendra J, Chenery AL, Parkinson JE, Chan BHK, Pearson S, Colombo SAP *et al.* IL-17A both initiates, via IFNγ suppression, and limits the pulmonary type-2 immune response to nematode infection. *Mucosal Immunol* 2020; **18**: 604.

52 Branchett WJ, Stölting H, Oliver RA, Walker SA, Puttur F, Gregory LG *et al.* A T cell-myeloid IL-10 axis regulates pathogenic IFN-γ-dependent immunity in a mouse model of type 2-low asthma. *J Allergy Clin Immunol* 2020; **145**: 666–678.e9.

53 Kelada SNP, Wilson MS, Tavarez U, Kubalanza K, Borate B, Whitehead GS *et al.* Strain-dependent genomic factors affect allergen-induced airway hyperresponsiveness in mice. *Am J Respir Cell Mol Biol* 2011; **45**: 817–824.

54 Walter DM, McIntire JJ, Berry G, McKenzie AN, Donaldson DD, DeKruyff RH *et al.* Critical role for IL-13 in the development of allergen-induced airway hyperreactivity. *J Immunol* 2001; **167**: 4668–4675.

55 Cook PC, MacDonald AS. Dendritic cells in lung immunopathology. *Semin Immunopathol* 2016; **38**: 449–460.

56 Gaurav R, Agrawal DK. Clinical view on the importance of dendritic cells in asthma. *Expert Rev Clin Immunol* 2013; **9**: 899–919.

57 McAlees JW, Lajoie S, Dienger K, Sproles AA, Richgels PK, Yang Y *et al.* Differential control of CD4(+) T-cell subsets by the PD-1/PD-L1 axis in a mouse model of allergic asthma. *Eur J Immunol* 2015; **45**: 1019–1029.

58 Silver FH, Freeman JW, Seehra GP. Collagen self-assembly and the development of tendon mechanical properties. *J Biomech* 2003; **36**: 1529–1553.

59 Xue M, Jackson CJ. Extracellular Matrix Reorganization During Wound Healing and Its Impact on Abnormal Scarring. *Adv Wound Care (New Rochelle)* 2015; **4**: 119–136.

60 Shoemaker CT, Reiser KM, Goetzman BW, Last JA. Elevated ratios of type I/III collagen in the lungs of chronically ventilated neonates with respiratory distress. *Pediatr Res* 1984; **18**: 1176–1180.

61 Bateman ED, Turner-Warwick M, Adelmann-Grill BC. Immunohistochemical study of collagen types in human foetal lung and fibrotic lung disease. *Thorax* 1981; **36**: 645–653.

62 Asgari M, Latifi N, Heris HK, Vali H, Mongeau L. In vitro fibrillogenesis of tropocollagen type III in collagen type I affects its relative fibrillar topology and mechanics. *Scientific Reports* 2017; **7**: 1392–10.

63 Kuivaniemi H, Tromp G. Type III collagen (COL3A1): Gene and protein structure, tissue distribution, and associated diseases. *Gene* 2019; **707**: 151–171.

64 Ritchie ME, Phipson B, Wu D, Hu Y, Law CW, Shi W *et al.* limma powers differential expression analyses for RNA-sequencing and microarray studies. *Nucleic Acids Res* 2015; **43**: e47.

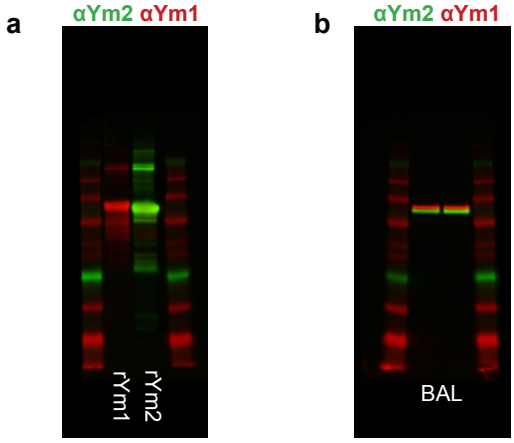

Supplementary Figure 1: Specificity of anti-Ym2
Specificity of anti-Ym1 and anti-Ym2 was analysed by western blot with **a**) total lysates expressing recombinant Ym1 and Ym2 or (**b**) BAL from C57BL/6 mice administered DRA allergens for 8 weeks. Ym1 and Ym2 protein was detected at ~48kDa.

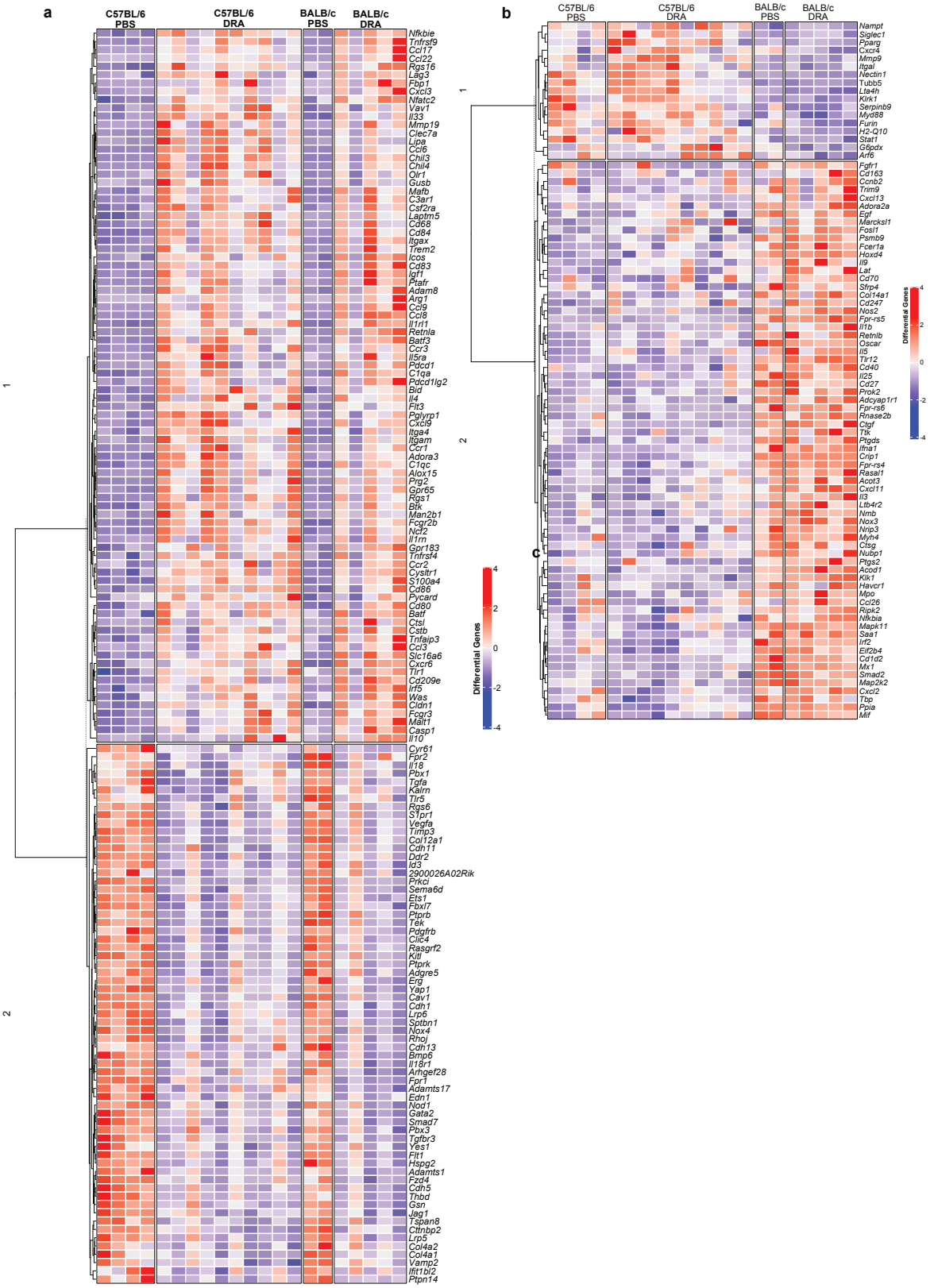

Supplementary Figure 2: Genes regulated in response to allergic inflammation in C57BL/6 and BALB/c mice. Whole lung RNA from C57BL/6 and BALB/c mice administered with either PBS or DRA for 8 weeks were analysed using NanoString Myeloid Panel v2. Unsupervised, hierarchically clustered heatmap of **a**) differentially expressed genes between PBS and DRA depicted for both mouse strains or **b**) genes that are differentially expressed between strains independently of allergen administration.